A Complex of Chaperones and Disulfide Isomerases Occludes the Cytosolic Face of the Translocation Protein Sec61p and Affects Translocation of the Prion Protein†

Jordan D. Stockton,‡ Matthew C. Merkert, and Kennan V. Kellaris*,§

Department of Chemistry, Georgetown University, Washington, D.C. 20007

Received June 25, 2003; Revised Manuscript Received September 8, 2003

ABSTRACT: Secretion of newly synthesized proteins across the mammalian rough endoplasmic reticulum (translocation) is supported by the membrane proteins Sec61p and TRAM, but may also include accessory factors, depending on the particular translocation substrate. Studies designed to investigate the binding of anti-peptide antibodies to the carboxyl terminus of the α-subunit of Sec61 (Sec61pα) lead us to the isolation of a complex of proteins that occlude the cytosolic face of Sec61pα in microsomes that have been prepared by standard protocols used to study translocation *in vitro* [Walter, P., and Blobel, G. (1983) *Methods Enzymol. 96*, 84−93]. This complex was shown by nanospray tandem mass spectrometry to be composed of protein disulfide isomerase (PDI), calcium binding protein 1 (CABP1/P5), 72 kDa endoplasmic reticulum protein (ERp72), and BiP (heat shock protein A5/HSPA5), and has been named TR-PDI for "translocon-resident protein disulfide isomerase complex". This constitutes a novel location for these proteins, which are known to be major constituents of the lumen of the rough endoplasmic reticulum. We have not established the function of TR-PDI at this location, but did observe that the absence of this complex results in a relative loss of correct topology of prion protein insertion across RER membranes, indicating the possibility of a functional role *in vivo*.

In eukaryotes, translocation of newly synthesized integral membrane and secretory proteins across the rough endoplasmic reticulum (RER)[1] is facilitated by a protein-conducting pore in the RER membrane termed the "translocon" (*2*). Nascent polypeptides that are destined for extracytoplasmic compartments or insertion into the membrane are synthesized on membrane-bound ribosomes (*3*). Ribosome−nascent chain complexes are targeted to the RER membrane by the signal recognition particle (SRP) after detection of signal sequences in the translocation substrate (*4*), and a tight junction is created between the ribosome and the integral membrane protein complex Sec61p (composed of α-, *β*-, and *γ*-subunits) (*5*).

The translocon membrane protein Sec61p forms the actual pore through which nascent translocating polypeptides pass (*5*−*7*). Sec61pα, -*β*, and -*γ*, in combination with the signal recognition particle (SRP) and the signal recognition particle receptor (SR), form a functional minimalist translocon that is sufficient to facilitate the translocation of several nascent substrate polypeptides across reconstituted lipid bilayers (*5*). Additionally, the translocon can include the 37 kDa membrane protein translocating chain-associated membrane protein (TRAM) (*7*), which is thought to regulate the interaction between a subset of nascent polypeptides and the membrane by preventing inappropriate partitioning into the lipid bilayer (*8*).

Optimal rates of translocation for many translocation substrates may depend on other "accessory" components that reside either in the lumen, in the cytoplasm, or as part of the membrane translocation complex itself under various circumstances (*9*). These include ribosome-associated membrane protein 4 (RAMP4), the translocon-associated protein (TRAP), and the oligosaccharyl transferase complex (OST) (*9*). Interestingly, the stoichiometric ratios of these assemblies appear to vary *in vivo*, perhaps to fulfill individual maturation requirements of different substrates. This indicates a highly dynamic set of component proteins that constitute the translocation apparatus, in a manner responsive to the identity of the particular translocation substrate.

The translocation machinery includes proteins that reside on the lumenal side of the RER membrane as well, including BiP, PDI, calnexin, calreticulin, GRP94, and ERp72 (*10*). These ensure unidirectionality of the transport process, detect aberrantly folded intermediates, and maintain the integrity of the bilayer by sealing the translocon pore (*11*).

In the studies reported here, anti-peptide antibodies created to bind to the carboxyl terminus of Sec61pα failed to bind to the cytosolic face of RER microsomes (the presumed location of the carboxyl terminus of Sec61pα). This initiated

† K.V.K. was supported as a Clare Boothe Luce Professor during a portion of this work.

* To whom correspondence should be addressed. E-mail: kellarkv@nature.berkeley.edu.

‡ Current address: Silicon Genetics, Redwood City, CA 94063.

§ Current address: Department of Plant and Microbial Biology, University of California, Berkeley, CA 94720.

[1] Abbreviations: SRP, signal recognition particle; RER, rough endoplasmic reticulum; RM, rough microsomes; RAMP4, ribosome-associated membrane protein 4; SR, SRP receptor; OST, oligosaccharyl transferase; TRAM, translocating chain-associated membrane protein; TRAP, translocon-associated protein; ERAD, ER-associated degradation pathway; BSA, bovine serum albumin; KLH, keyhole limpet hemocyanin; SB, 0.4 M sucrose, 0.4 M KOAc, 20 mM Tris-OAc (pH 7.6), 1 mM EDTA, and 1.5 mM $MgOAc_2$; KRM, potassium-washed RM; NaKRM, sodium- and potassium-washed RM; ApoB, apolipoprotein B; PrP, prion protein; pPL, preprolactin; VSVG, vesicular stomatitis virus glycoprotein; TR-PDI, translocon-resident protein disulfide isomerase complex; AP, competitive acceptor tripeptide for N-linked glycosylation.

10.1021/bi035087q CCC: $25.00
Published on Web 10/17/2003

a series of experiments that ultimately led to the discovery of a complex of cytosolic proteins that occlude Sec61pα in these translocationally active mammalian RER microsomes. Three members of this protein complex are previously identified members of the protein disulfide isomerase family; the fourth is BiP. We have named this complex the translocon-resident protein disulfide isomerase complex (TR-PDI).

After screening many translocation substrates for sensitivity to the presence or absence of TR-PDI, we observed a noticeable effect of TR-PDI on the translocation of the prion protein. We found that this substrate displays visibly different insertion behaviors across RER microsomes that either have TR-PDI bound to the cytosolic surface or that have been washed of TR-PDI by very mild detergent treatment (0.01−0.05% detergent). This behavior was partially or completely reversed by re-addition of purified TR-PDI.

We propose that TR-PDI may carry out a chaperone-like role in the translocation process from the cytosolic side of the translocon.

EXPERIMENTAL PROCEDURES

Anti-Peptide Antibodies. Antiserum against the carboxyl terminus of Sec61pα (anti-Sec61pαC) has been previously described (*12*). Briefly, the NH_2-Cys-Lys-Glu-Gln-Ser-Glu-Val-Gly-Ser-Met-Gly-Ala-Leu-Leu-Phe-COOH peptide was cross-linked to BSA and used to produce anti-peptide antibodies in New Zealand white rabbits. This 15mer, with the exception of the N-terminal cysteine that was incorporated for cross-linking purposes, reflects the 14-amino acid carboxyl terminus of Sec61α. The antiserum was used directly from the supernatant of coagulated blood samples, without further purification.

The antisera against the 54 kDa subunit of SRP (anti-SRP54) were generated against the NH_2-Cys-Asp-Thr-Ser-Gly-Arg-His-Lys-Gln-Glu-Asp-Ser-COOH 12mer cross-linked to keyhole limpet hemacyanin (KLH) and used to elicit an immune response in New Zealand white rabbits. This 12mer, except for the N-terminal cysteine residue which was incorporated for cross-linking to the carrier protein, corresponds to a region near the GTP binding site in the SRP54 subunit. This peptide was chosen because it is predicted to form a loop structure on the surface of the folded protein, and its high charge content was predicted to be able to elicit a strong immunogenic response. The antiserum recognizes SRP in its native, membrane-bound state.

Coupling of IgG to Protein A−Sepharose Beads. Anti-Sec61pαC and anti-SRP54 antibodies were covalently coupled to protein A−sepharose CL-4B beads (Sigma, St. Louis, MO) as described by Harlow (*13*) to create antibodies that were physically constrained to the surface of a solid support rather than free in solution. Briefly, a 50% (v/v) suspension of protein A−Sepharose CL-4B beads was washed twice with phosphate-buffered saline. The beads were resuspended in an equal volume of antisera and were allowed to incubate for 90 min at room temperature with end over end rotation. After incubation, the beads were washed twice with 10 volumes of 200 mM sodium borate (pH 8.0), resuspended in 10 volumes of 20 mM dimethylpimelimidate (Sigma), and gently agitated for 1 h at room temperature. The reaction was quenched with two washes in 200 mM triethylamine (pH 9.0), followed by incubation for 2 h in the same buffer. The beads were then washed once with phosphate-buffered saline, twice with 100 mM glycine (pH 2.8), and twice more with phosphate-buffered saline to remove the majority of unbound IgG.

Preparation of NaKRM. Rough microsomes (RM) were prepared from canine pancreas as described by Walter and Blobel (*1*). Where reported, these microsomes were further stripped with washes with high concentrations of sodium and potassium as follows. Microsomes (1000 equiv/mL) were diluted with an equal volume of 250 mM sucrose, 50 mM triethanolamine acetate (TEA) (pH 7.4), 1 mM DTT, and 50 mM EDTA (pH 7.6) and were incubated on ice for 20 min. Membranes were then pelleted by centrifugation in a Beckman Ti50.2 rotor for 1 h at 44 000 rpm over a cushion of 0.5 M sucrose, 50 mM TEA, and 1 mM DTT. Pellets were washed three times in 500 mM potassium acetate, 5 mM magnesium acetate, 250 mM sucrose, 25 mM TEA, and 1.0 mM DTT followed by centrifugation in a Beckman Ti50.2 rotor for 1 h at 40 000 rpm over the cushion described above. These membranes were resuspended to their original volume in 250 mM sucrose, 50 mM TEA, and 1 mM DTT and pelleted over a cushion containing 500 mM sucrose and 50 mM TEA for 12 min at 30 psi in an A-100/30 rotor using a Beckman Airfuge (Beckman Instruments, Inc., Fullerton, CA). For highly stringent washes, the pellet was resuspended in 3 M NaCl and 10 mM sodium phosphate (pH 7.6), incubated on ice for 20 min, and centrifuged for 8 min at 30 psi (without cushion). This extensively washed pellet contains sealed, right-side-out ER microsomes, and is termed the NaKRM pellet. It is competent for translocation in a wheat germ translation system with the addition of exogenous SRP.

Immunoglobin Binding Assays. The amount of anti-Sec61pαC that bound to the Sec61pα carboxyl terminus was determined as follows. Sodium- and potassium-washed RER microsomes (NaKRM) derived from 50 equiv of RM were resuspended in 50 μL of phosphate-buffered saline containing various concentrations of the mild ionic detergent sarkosyl (Calbiochem, La Jolla, CA), as indicated. After incubation for 30 min at 4 °C, each sample was supplemented with 25 μL of antiserum against the Sec61pα carboxyl terminus (anti-Sec61pαC), and allowed to incubate on ice for 2 h. The tubes were centrifuged for 12 min at 30 psi in a Beckman A-100/30 rotor, and the pellets, containing NaKRM and any bound IgG, were resuspended in their original volume of phosphate-buffered saline and sarkosyl. The microsomes were centrifuged a second time at 30 psi for 12 min to remove nonspecifically bound proteins.

The bound IgG was then eluted from the microsomal pellet by washing the microsomes with a 3 M NaCl, 10 mM NaH_2PO_4, pH 7.6 buffer. After recentrifugation, the supernatants containing the eluted IgGs were collected and incubated with 25 mL of a 50% (v/v) suspension of protein A−Sepharose CL-4B beads to quantitatively bind the IgG fraction. The beads were then washed twice in phosphate-buffered saline, treated with 0.33 M Tris base, 8.3% SDS, and 0.33 M DTT (SDS-reduction mix) to elute bound IgG, and the eluate was loaded onto a 12% SDS−PAGE gel for separation.

Measurement of the amount of anti-Se61pαC that was able to bind cholate-stripped microsomes was accomplished similarly. NaKRM pellets derived from 50 equiv of RM were

resuspended in 50 μL of sucrose buffer [0.4 M sucrose, 0.4 M potassium acetate, 20 mM Tris-acetate (pH 7.6), 1 mM EDTA, and 1.5 mM magnesium acetate] containing sodium cholate at the indicated concentrations. The microsomes were centrifuged for 12 min at 30 psi in a Beckman A-100/30 rotor and the pellets resuspended in SB without added sodium cholate. After incubation for 30 min at 4 °C, each sample was supplemented with 10 μL of anti-Sec61pαC antiserum, and the tubes were incubated on ice for 2 h. The microsomes, with bound IgG, were recentrifuged as described above, and the pellets were gently rinsed with 200 μL of SB, resuspended in 50 μL of SB, and recentrifuged. The previous washing, resuspension, and centrifugation step was repeated, after which the pellet was resuspended in 50 μL of SDS-reduction mix. Ten microliters of each sample was separated on a 4 to 12% Bis-Tris acrylamide gel (Novex, Frankfurt, Germany) to allow quantitation of the successfully bound anti-Sec61pαC IgG.

Microsome Immunoprecipitation Assay. To determine the level of anti-Sec61pα antibody binding that is restricted to the cytosolic face of microsomes, an inverse binding assay was devised. NaKRM pellets derived from 175 equiv of RM were resuspended in 175 μL of either 0, 0.005, 0.01, 0.05, 0.1, or 0.2% (w/v) sarkosyl in phosphate-buffered saline and incubated for 30 min on ice. A 25 μL suspension of either anti-Sec61pαC−protein A−Sepharose or anti-SRP54−protein A−Sepharose beads was added to each detergent-treated NaKRM sample, and the tubes were allowed to incubate at 4 °C for 2 h with end over end rotation, followed by settling of the IgG−protein A−Sepharose beads at room temperature for 20 min. The supernatant containing unbound microsomes was gently removed from the beads using capillary pipet tips. The beads were then gently washed three times with phosphate-buffered saline, allowing them to settle without centrifugation between each wash. Microsomes that were able to bind to IgG tethered to protein A−Sepharose beads (thus restricting interactions to the exposed cytosolic face) were dissolved in SDS-reduction mix and quantitated after separation of the microsomal proteins on 12 to 20% acrylamide gels. Microsomes pelleted via their interaction with either anti-Sec61pαC or anti-SRP54 were quantitated by Western blotting using polyclonal antisera against the 48 kDa subunit of oligosaccharyl transferase (*14*) as a marker protein, allowing quantitation of pelleted, intact RER microsomes.

SDS−PAGE, Immunoblotting, and Quantitation of Gel Products. Protein preparations were precipitated with 10% trichloroacetic acid, resuspended in SDS-reduction mix, and incubated at 55 °C for 30 min. Gel loading buffer (0.3 M DTT, 50% glycerol, and 0.01% bromophenol blue) was then added to each sample, followed by incubation at 100 °C for 2 min. Proteins were analyzed by SDS−PAGE on either 12%, 12 to 20% Tris-glycine, or 4 to 20% Bis-Tris precast Novex polyacrylamide gradient gels (Novex, San Diego, CA), as indicated. The composition of the fractions from the purification of TR-PDI was determined by silver staining, using the method of Rabilloud (*15*).

Immunoblots were performed by transferring SDS−PAGE-separated proteins onto Immobilon-P PVDF membranes (Millipore, Bedford, MA) using a semidry transfer apparatus (Bio-Rad, Emeryville, CA). Tris-glycine gels were transferred using a 25 mM Tris, 192 mM glycine, pH 8.0 buffer at 17 V for 0.6 h; Bis-Tris gels were transferred using a 25 mM Bicine, 25 mM Bis-Tris, 1 mM EDTA, pH 7.2 buffer at 30 V for 1 h.

For the immunoglobin binding assays, blots were developed by incubating the PVDF membranes with secondary antibody alone (horseradish peroxidase-coupled goat anti-rabbit IgG at a 1:50000 dilution; Sigma) to quantitate bound IgG. For the inverse microsome immunoprecipitation assays, the harvested microsomal proteins were transferred from 12% SDS−PAGE gels to PVDF membranes and incubated with anti-OST48 antibodies (1:25000 dilution), followed by incubation with horseradish peroxidase-coupled goat anti-rabbit IgG secondary antibody. In all cases, peroxidase-coupled secondary antibodies were detected using enhanced chemiluminescence (ECL) (Pierce, Rockford, IL) and Kodak X-Omat film. Densitometry of Western blots was performed using the Quantity One program (version 2.7) from Protein + Dna ImageWare Systems (Huntington Station, NY).

Preparation of ChoRM. To strip membranes of TR-PDI, rough microsomes were first washed with 10 mM EDTA to remove bound ribosomes. The 120000*g* pellet from this wash was subsequently washed three times with 500 mM KOAc and then once with 3 M NaCl to remove SRP, remaining ribosomes, and many other weakly bound membrane-associated proteins. The resulting pellet was suspended in 0.05% (w/v) cholate in SB buffer [0.4 M sucrose, 0.4 M potassium acetate, 20 mM Tris-acetate (pH 7.6), 1 mM EDTA, and 1.5 mM magnesium acetate], incubated on ice for 30 min, and recentrifuged. The membranes were resuspended in SB without added cholate and repelleted, and the resulting membrane fraction was suspended in SB and used for subsequent translocation assays as ChoRM microsomes.

Reconstitution of TR-PDI onto Cholate-Washed Microsomes. Reconstitutions were carried out as follows. First, 0.05% cholate-stripped ChoRM (4 equiv/μL) were mixed with 2 volumes of purified TR-PDI and 7 volumes of 50 mM TEA (pH 7.6) and 1 mM DTT. The samples were gently mixed and allowed to incubate at 4 °C for 90 min, followed by centrifugation for 12 min at 22 psi in a Beckman A-100/30 rotor. Pelleted membranes thus reconstituted with TR-PDI were resuspended in 50 mM TEA (pH 7.6), 250 mM sucrose, and 1 mM DTT for use in translation assays.

Purification of the Translocon-Resident Isomerase Complex. A 0.05% cholate extract was prepared from 40 000 equiv of NaKRM by resuspending NaKRM in 40 mL of sucrose buffer [0.4 M sucrose, 0.4 M potassium acetate, 20 mM Tris-acetate (pH 7.6), 1 mM EDTA, and 1.5 mM magnesium acetate] containing 0.05% sodium cholate. The microsomes were sedimented at 120000*g*, and the pellets were resuspended in SB without added sodium cholate. The supernatant was concentrated to 2 mL and exchanged with 10 mL of 20 mM TEA (pH 7.6) and 0.01% (w/v) sodium cholate using an Amicon microconcentrator equipped with a YM-10 membrane (Millipore). This concentrated, low-salt sample was loaded onto a Pharmacia Mono-Q HR-5 ion exchange column (Pharmacia, Piscataway, NJ). The column was washed with 4 mL of 0.01% (w/v) sodium cholate and 20 mM TEA (pH 7.6), followed by elution with a 30 mL linear gradient of sodium chloride (from 0.0 M NaCl, 3 mL of 350 mM NaCl, 23 mL of 550 mM NaCl, and 30 mL of 1 M NaCl). Fractions (1 mL) were collected and assayed

for their ability to re-occlude the Sec61pα carboxyl-terminal epitope. The fraction most highly active in re-occlusion of the Sec61pα epitope after reconstitution onto detergent-washed microsomes (eluting at 9 mL) was exchanged with 10 mL of SB containing 0.01% (w/v) sodium cholate, and the volume was reduced to 0.5 mL using an Amicon YM-10 membrane as described above. A portion of the fraction that was able to re-occlude the Sec61pα epitope was processed for sequencing, as outlined below. The remainder was loaded onto a Pharmacia Superose 12 size exclusion column (Pharmacia) and eluted with SB at a flow rate of 0.4 mL/min to determine the homogeneity of the complex.

Cell-Free Translations. Wheat germ cell-free translations and proteinase K assays were performed as described previously (*16*) using [^{35}S]methionine (Amersham) to visualize translation products via fluorography. Transcription and translation experiments were carried out as described by Gilmore and co-workers (*17*) using either PG_4BP_4, containing a full-length clone of the bovine prolactin gene (*18*), or pG3G, encoding vesicular stomatitis virus glycoprotein (VSVG) (*19*) (both courtesy of R. Gilmore, University of Massachusetts, Worcester, MA), EB17 encoding apolipoprotein B (*20*), pAV3 encoding prion protein with mutations encoding three alanine-to-valine substitutions at positions 113, 115, and 118, and MH2MPrP encoding the native prion protein (*21*, *22*) (EB17, pAV3, and MH2MPrP courtesy of V. Lingappa, University of California, San Francisco, CA). Plasmids were first linearized as described previously (*17*), and preparative-scale transcription reactions were performed following the protocol of Gürevich and co-workers (*23*).

Total canine kidney messenger RNA was isolated from flash-frozen kidney tissue using urea extraction and an oligo-dT column (Sigma) as described in Current Protocols in Molecular Biology (*24*).

Translations were supplemented with the various microsomal preparations described herein, as well as purified SRP where indicated. SRP was purified by following the protocol of Walter and Blobel (*1*).

Sequencing. Members of the purified complex that were found to re-occlude the carboxyl terminus of Sec61pα were separated on a 4 to 12% Bis-Tris SDS−PAGE gel and were visualized by staining briefly with Coomassie brilliant blue and destaining with 10% MeOH and 15% acetic acid. Bands were excised from the gel and sent to the Harvard Microchemistry Facility (Cambridge, MA) where they were subjected to in-gel trypsin digestion. The resulting proteolytic peptides were separated by microcapillary reverse-phase HPLC coupled to a nano-electrospray tandem mass spectrometer on a Finnigan LCQ quadropole ion trap mass spectrometer (*25*). MS/MS spectra were correlated with known sequences using the Sequest algorithm (*26*), and identities were confirmed by manual analysis of results.

Radiography. For *in vitro* translations, [^{35}S]methionine-labeled gels were visualized by fixation of the SDS−PAGE gel in acetic acid and impregnation with poly-phenyl-oxazole (PPO, 10% in acetic acid), followed by drying of the gel and exposure to Kodak X-Omat AR film at −80 °C.

Densitometry of ^{35}S flourographs was performed using the Quantity One program (version 2.7) from Protein + Dna ImageWare Systems.

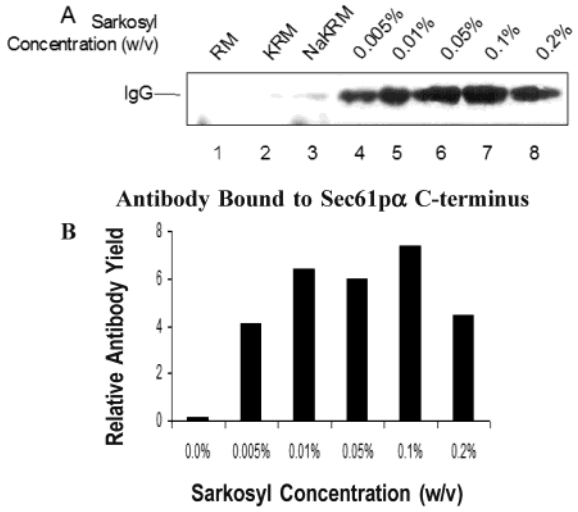

FIGURE 1: Carboxyl terminus of Sec61pα which becomes accessible to antibodies upon treatment with sarkosyl. (A) Western blot visualizing the amount of anti-Sec61pα carboxyl-terminal IgG that cosediments with detergent and salt-washed microsomes after various detergent treatments. The bound IgG-labeled microsomes were pelleted, solubilized, and separated on 12% SDS−PAGE gels for quantitation. The amount of bound IgG was measured by Western blotting with secondary antibody (peroxidase-coupled goat anti-rabbit IgG) and quantified by scanning densitometry. Lanes 1−3 show relative amounts of the antibody that binds to native RM, potassium-washed RM (KRM), and potassium- and sodium chloride-washed RM (NaKRM), respectively. Lanes 4−8 depict the amount of antibody that binds to NaKRM that have been washed with varying amounts of sarkosyl, ranging from 0.005 to 0.2% (w/v). (B) Relative yield of anti-Sec61pα carboxyl-terminal IgG that pellets with the microsomes in the various detergent solutions as quantitated by scanning densitometry.

RESULTS

The Carboxyl Terminus of Sec61pα Is Inaccessible to Antibodies. These studies began by attempting to accurately determine the transmembrane orientation and accessibility of the carboxyl terminus of Sec61pα in sealed, translocation-competent RER membranes. Anti-Sec61pαC antisera (directed against the carboxyl-terminal sequence of Sec61pα, NH_2-CKEQSEVGSMGALLF-COOH) bind with high affinity to Sec61pα on immunoblots (useful at a 1:40000 dilution). However, we were unable to bind measurable amounts of antibody to natively symmetric (cytosolic side out) rough microsomes (RM), even after co-incubation of RM with a high concentration of antisera over a period of several hours (Figure 1A, lane 1). Further, stripping of ribosomes from the rough endoplasmic reticulum (RER) via treatment with 50 mM EDTA followed by 500 mM potassium acetate did not measurably improve antibody binding (Figure 1A, lane 2). Even stringent washing of the microsomal membranes with NaCl did not measurably improve the accessibility of the IgG antibody pool to the Sec61pα epitope (Figure 1A, lane 3).

We first explored the possibility that the carboxyl terminus of mammalian Sec61pα is on the lumenal side of the membrane, despite previously reported results which indicated the carboxyl terminus of yeast Sec61pα is cytosolic (*27*). First, we treated the stringently washed RM (NaKRM) with increasing amounts of the detergent sarkosyl to permeabilize the microsomes, giving antibodies access to both sides of the membrane. Enhanced binding would indicate

either that the carboxyl terminus lies on the lumenal side of the ER membrane or, alternatively, that the detergent perturbs the accessibility of Sec61pα on the cytosolic side, thereby exposing a previously hidden epitope.

Native RM, KRM, and NaKRM (all containing Sec61p) bind nearly undetectable levels of the anti-Sec61pαC IgG component from the antiserum (Figure 1A, lanes 1−3); in contrast, even low concentrations of sarkosyl significantly improve the ability of microsomes to recognize and bind the anti-Sec61pαC IgG (Figure 1A, compare lanes 1−3 to lanes 4−8).

The Carboxyl Terminus of Sec61pα Is Cytosolic. To determine whether the newly revealed Sec61pα carboxyl terminus is on the cytosolic or lumenal face of RER microsomal membranes, we devised a novel microsome immunoprecipitation assay, using anti-Sec61pαC antibodies covalently linked to protein A−Sepharose beads via their IgG constant region (*13*). We reasoned that the distance between the IgG variable region and the Sepharose bead would be insufficient to span the width of the membrane. These "tethered" antibodies should be unable to bind to epitopes that reside on the lumenal face of the ER membrane, even after membrane permeabilization.

After sarkosyl treatment, entire RER microsomes were sedimented using these Sepharose−protein A−IgG beads, and quantitated using antisera directed against the 48 kDa subunit of the oligosaccharyl transferase complex (αOST48). OST48 is a ubiquitous integral membrane protein in the RER, and is used here to measure the relative yield of intact microsomes pelleted via the Sec61pα antigen−antibody interaction. As a control, we also carried out microsome immunoprecipitations using a protein A−Sepharose assembly linked to antibodies directed against the 54 kDa subunit of the signal recognition particle (SRP54), which is native to the cytosolic face of RER microsomes. Note that if the occlusion phenomenon is an artifact due to redistribution of chaperone-like occluding factors on the RER microsomal surface during microsomal preparation, this epitope would be expected to be occluded as well.

In Figure 2, the amount of OST48 visualized by Western blotting was used to quantitate the total pelleted microsomal pool in each sample. Microsomal membranes were pelleted either via interaction with αSRP54 antibody (Figure 2A) or with αSec61C antibody (Figure 2B) cross-linked to the protein A−Sepharose beads. We allowed the chemiluminescent reaction of the horseradish peroxidase-coupled secondary antibody to overexpose the film (Figure 2A). This was done to ensure visualization of OST48 across a wide range of concentrations. Our purpose was to detect even minimal binding to the Sec61pα epitope, to determine conditions under which Sec61pα is fully occluded.

In panel B, it can be seen that microsomes are pelleted via the anti-Sec61pαC IgG−protein A−Sepharose interaction only after mild detergent washing of the microsomes, reaching a maximum at ∼0.1% (w/v) sarkosyl. In contrast, microsome pelleting using anti-SRP54 antibodies was maximal prior to detergent treatment, and exhibited a slow but steady decrease as the detergent concentration increased. We conclude that the interaction between IgG and the carboxyl terminus of Sec61pα occurs on the cytosolic face of the ER, and is greater as levels of sarkosyl approach 0.1%. Exposure of the SRP54 epitope required no prior detergent treatment,

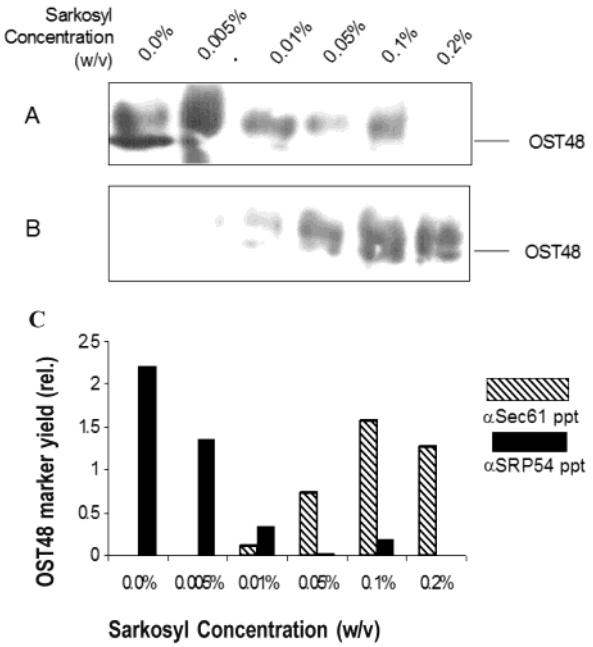

FIGURE 2: Tethered antibodies bind to the carboxyl terminus of Sec61pα on the cytosolic face of the ER membrane. The change in antibody accessibility of Sec61p after detergent washing is compared with that of the accessibility of the well-characterized membrane-associated signal recognition particle (SRP). Anti-SRP54 antibodies (A) or Anti-Sec61pα carboxyl-terminal antibodies (B) were coupled to 0.1 mm polystyrene beads and used to pellet detergent-washed microsomes via antibody−epitope conjugation. The pelleted microsomes were then separated on a 12% SDS−PAGE gel, and the total microsomal yield was quantitated using anti-OST48 antibodies followed by ECL detection. The relative yield of OST48 (C), and thus pelleted microsomes, was quantitated by scanning densitometry of the OST48 band from the Western blots shown in panels A and B.

indicating that SRP54 resides on the cytosolic face of these membranes, and is fully accessible prior to detergent treatment. This further indicates that these membranes are well-behaved, and there is no general occlusion of the microsomal surface due to artifactual reorganization during our microsomal preparation and washing protocols.

Our use of antibodies for two distinct phases of the immunoprecipitation and detection steps leads to two distinct antibody bands on the SDS−PAGE gels depicted in Figure 2A. The lower bands are due to primary antibody binding to the OST48 protein, followed by development with secondary antibody using standard Western blot procedures. The upper bands, however, are due to IgG in the microsomal protein pool itself. This band reflects IgGs used to pellet the microsomes (via binding to Sec61pα) that do not remain covalently linked to the protein A−Sepharose beads, because the cross-linking reaction is less than 100% efficient.

The increasing background IgG level commensurate with the amount of microsomes successfully pelleted is reflected by the coordinated yield of background IgG and OST48 (upper vs lower bands, Figure 2A). The unusual nature of this protocol, along with overexposure of the chemiluminescence reaction, produced the broad banding patterns visible in Figure 2A.

To establish the relative extent of occlusion of the carboxyl terminus of Sec61p, we used NaKRM microsomes to bind the anti-Sec61pα antibody from a 140 μL aliquot of antisera. We compared the amount of IgG that successfully bound to

Sec61pα in the membranes from this large pool to the amount of IgG from a much smaller aliquot (1.5 μL) that was able to bind Sec61pα on a Western blot. The total amount of IgG that bound to the microsomes from the 140 μL pool produced less than <1% of the IgG binding available in the much smaller (1.5 μL) pool, suggesting that the rough microsomes bind less than 0.01% of the available Sec61pα specific antibody prior to mild detergent washing (data not shown).

The stringent washes prior to this binding assay indicate that the lack of binding of Sec61pα antisera is not due to a small subset of microsomes that have been rendered leaky during the freeze−thaw cycle, as the washes occurred after thawing; further, the behavior (lack of measurable IgG binding) is observed for the entire population.

We next tested several other possibilities: (1) that sarkosyl denatures the carboxyl-terminal region of Sec61pα, creating a more accessible epitope with greater antibody binding avidity, (2) that antibody binding is an artifactual phenomenon in which the permeabilized membranes trap a fraction of the antibodies in the now-accessible lumen, or (3) that an as yet uncharacterized factor covers the antigenic epitope of Sec61pα, and is removed by mild detergent treatment.

The Carboxyl Terminus of Sec61pα Is Occluded by a Cytosolic Factor. To rule out the possibility that antibody binding on the cytosolic face is due to a large increase in antibody affinity for the denatured form of the Sec61pα carboxyl terminus, we subjected detergent-washed microsomes to conditions known to facilitate protein renaturation. Exhaustive dialysis as well as detergent adsorption with macroporous polystyrene beads did not measurably reduce the level of binding of antibodies to the Sec61pα C-terminal epitope (data not shown), suggesting that enhanced exposure was the result of the removal of an occluding factor rather than the result of an unfolding event.

We next looked for a mild detergent that would allow successful re-occlusion of the Sec61pα carboxyl terminus from the detergent extract, reasoning that if an occluding factor was responsible, we would need to be able to specifically reverse this exposure to purify the putative factor(s). Of the detergents tested (CHAPs, deoxyBigCHAP, cholate, and β-octyl glucoside), only cholate was found to support reversible exposure of the carboxyl terminus of Sec61pα.

Maximum binding of IgG to the Sec61pα carboxyl-terminal epitope was seen after treatment of NaKRM with an extremely mild (0.01%, w/v) sodium cholate solution (Figure 3, lane 3). Importantly, we were able to reconstitute epitope occlusion by adding the cholate extract back to the detergent-washed microsomes, followed by a 3-fold dilution with buffer (Figure 3, lane 7), indicating the occluding factor was in the cholate extract, and binding was reversible. This behavior allowed us to purify the factor responsible for occlusion of Sec61pα.

Purification of the Sec61pα Carboxyl-Terminal Occluding Factor. The supernatants from increasing concentrations of cholate treatment were analyzed by SDS−PAGE. As seen in Figure 4, the extracts from salt-washed microsomes at 0.005, 0.01, or 0.05% sodium cholate contain a fairly small subset of proteins compared to those remaining with the membrane fraction (10−12 proteins, appearing as the darker stained bands; Figure 4, lanes 3, 5, and 7). With 0.1% cholate,

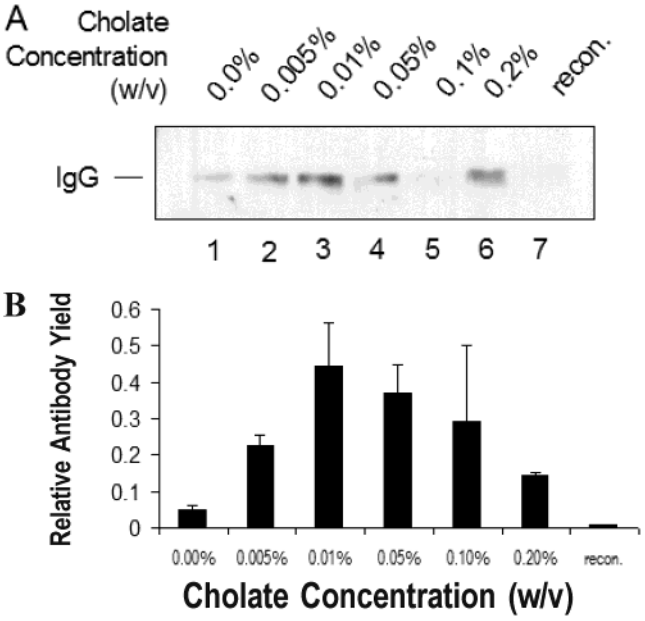

FIGURE 3: Carboxyl terminus of Sec61pα which becomes accessible to antibodies upon treatment with sodium cholate. (A) Anti-Sec61pα carboxyl-terminal antibody bound to NaKRM microsomes after cholate washing. Rebinding of the cholate-extracted factor(s) responsible for Sec61pα occlusion was realized by reconstituting the membrane fraction from a 0.05% cholate wash with a 10×, detergent-depleted extract of the 0.05% cholate supernatant. Lane 7 contained a reconstituted membrane fraction that was exposed to anti-Sec61α antibodies as in lanes 1−6. Ten equivalents of each membrane fraction was separated on a 4 to 12% Bis-Tris acrylamide gel. (B) The relative yields of IgG that bound to the carboxyl terminus of Sec61α from three such assays were quantitated by scanning densitometry.

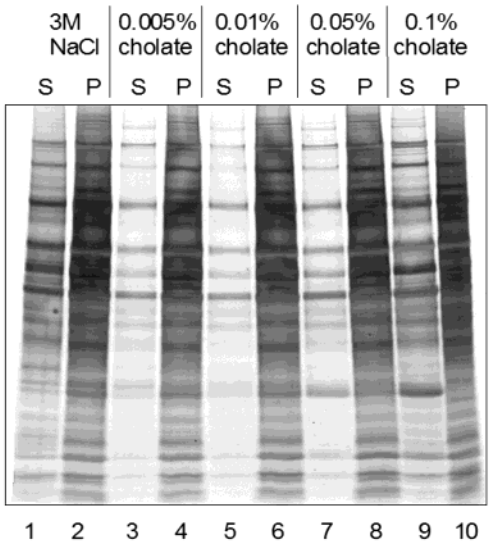

FIGURE 4: Cholate extract (0.05%) contains a select, membrane-associated set of proteins. Potassium-washed microsomes (3× KRM) were washed with a solution containing 3 M NaCl and then sedimented at 120000*g*. The supernatant (S) and pellet (P) are shown in lanes 1 and 2, respectively. Pellets were resuspended in buffer containing 400 mM potassium acetate at various sodium cholate concentrations. The supernatants and pellets from each extraction are shown in lanes 3−10. Each pair of lanes represents the total protein from 2 equiv of membranes, visualized by Coomassie staining.

the supernatant contains many more proteins (approximately 40−50 visible overlapping bands; Figure 4, lane 9), indicating that at this higher cholate concentration the integrity of

the sealed microsomal membranes is breached. Access to lumenal proteins in these canine endoplasmic reticulum microsomes, we conclude, does not occur until treatment with 0.1% cholate, a concentration of cholate 10-fold higher than that necessary to remove the occluding factor from the cytosolic face of Sec61pα. This behavior is in agreement with previous findings, in which lumenal proteins begin to appear in the supernatant of pelleted ER microsomes treated with ≥0.2% cholate (ref *28* and personal communication from C. Nicchitta). The slight difference in cholate concentration (0.1% reported here vs release between 0.13 and 0.2% cholate in Nicchitta's hands) is most likely due to slight differences in buffer, and therefore salt, concentrations. We also observed that the microsomal pellet from the 0.1% cholate extract is noticeably smaller than the pellets from any of the extractions at lower cholate concentrations. Further evidence supporting the integrity of microsomes washed with <0.1% cholate includes the protein A−Sepharose microsome pelleting results (Figure 2), in which OST48 copellets with Sec61p, indicating an intact microsomal membrane. Treatment of the NaKRM microsomes with cholate concentrations of ≤0.01% had no effect on translocation efficiency (as measured by the proteinase K accessibility of signal peptide-cleaved, full-length PL), while higher concentrations of detergent (≥0.1%) had a drastic effect on translocation efficiency, with the nearly complete loss of both signal sequence processing and occlusion in the ER lumen (data not shown). Treatment of membranes with the other detergents (CHAPs, deoxyBigCHAP, and β-octyl glucoside) resulted in the complete loss of the ability to support translocation *in vitro*.

Sec61pα Is Occluded by a Complex of BiP, PDI, and PDI-like Proteins. To identify the component(s) of the extract responsible for Sec61pα epitope occlusion, we purified the occlusion factor from the concentrated extract of the 0.05% cholate strip (Figure 4, lane 7) by ion exchange chromatography on a Mono-Q HR-5 column. Column eluates were assayed for their ability to re-occlude the Sec61pα epitope after removal of the cholate detergent. The fractions affording the highest level of occlusion (panels A and B of Figure 5, fractions 8 and 9) contain varying amounts of four bands: two proteins displaying an apparent mass of approximately 72 kDa, a 58 kDa protein, and a 52 kDa protein. The proteins in fraction 9 from the Mono-Q eluate were further subjected to size exclusion chromatography on a Superose 12 column (Figure 6). These four proteins behave as a single species during size exclusion chromatography, eluting in a single size exclusion fraction (Figure 6, fraction 12). We therefore refer to this set of four proteins as a complex, though we feel the constitution of this complex may be highly dynamic.

The members of the complex were sequenced by the Harvard Microchemistry Facility using mass spectrometry of peptides generated from in-gel digestion of the individual proteins separated by SDS−PAGE. They were identified as human protein disulfide isomerase-related P5 protein CABP1 (P5, GI:1710248) at 52 kDa, protein disulfide isomerase (PDI, GI:129726) at 58 kDa, and human 72 kDa protein disulfide isomerase-related protein (ERp72, GI:4758304) and BiP (GI:109893) at 72 kDa. The identified sequences from the 52 kDa CABP1/P5 protein include a peptide from the amino-terminal putative signal sequence of this protein.

Given that this complex is composed primarily of members of the protein disulfide isomerase family, we have named this complex the translocon-resident protein disulfide isomerase complex (TR-PDI).

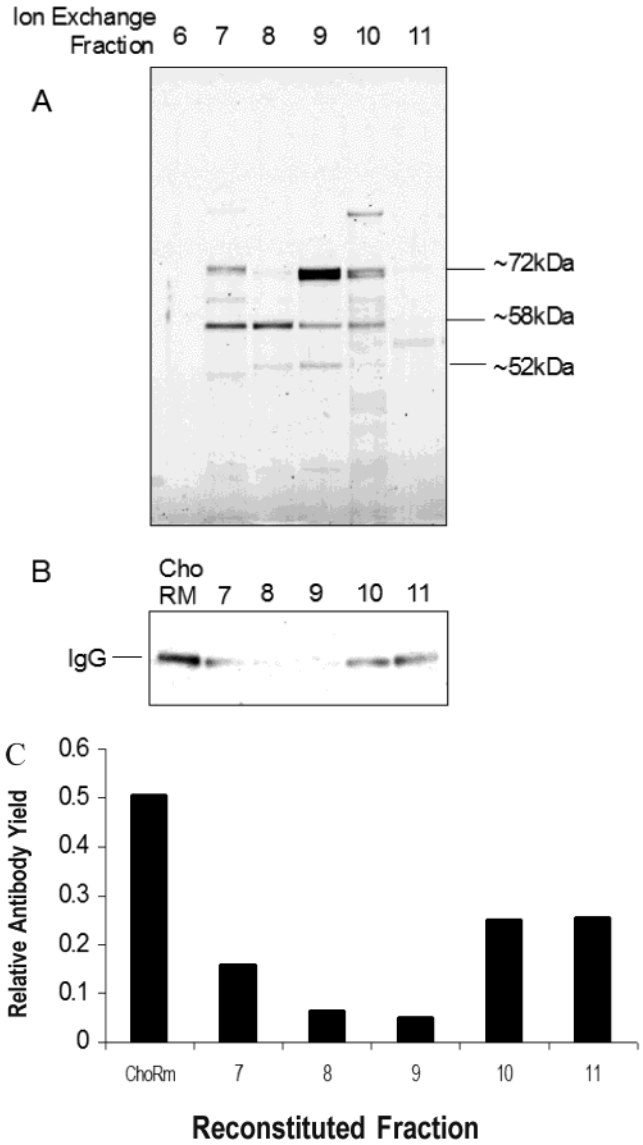

FIGURE 5: Ion exchange separation of the 0.05% cholate wash to identify factors capable of occluding the Sec61pα carboxyl terminus. (A) The 0.05% (w/v) cholate extract from salt-washed rough endoplasmic microsomal membranes was fractionated via anion exchange chromatography on a Mono-Q column. All fractions were tested for their ability to reconstitute Sec61pα occlusion when reconstituted onto cholate-stripped microsomes. Those fractions displaying the greatest ability to re-occlude Sec61pα were separated via SDS−PAGE and stained with Coomassie. (B) Occlusion activity is measured by SDS−PAGE separation and secondary antibody detection of anti-Sec61pα IgG antibodies that are bound to cholate-washed microsomes. A portion of each fraction was diluted 3-fold and added back to microsomes previously extracted with 0.5% cholate to assess occlusion of Sec61pα. (C) Relative yield of each sedimentation assay as quantitated by scanning densitometry.

Activity of TR-PDI. Our data indicate that the anti-Sec61p epitope, and at least a portion of the TR-PDI occluding complex, are cytosolic; it follows that this complex is close to the ribosome−Sec61 junction and the site of translocation. We wondered, therefore, if TR-PDI may be involved in some aspect of the translocation process. To test this, we first asked whether TR-PDI affects basal translocation for a well-characterized translocation substrate, preprolactin. We also asked if TR-PDI might be capable of chaperone-like function,

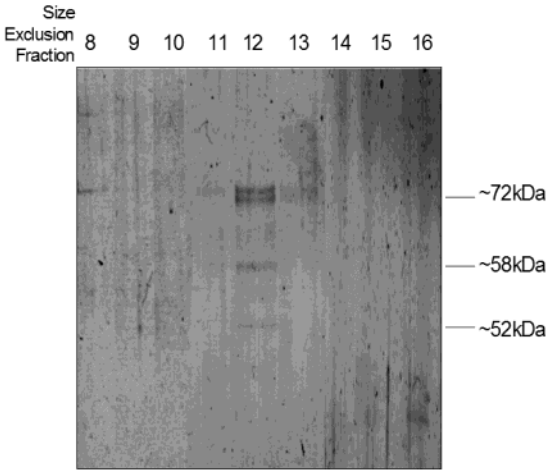

FIGURE 6: Size exclusion separation of the Sec61pα carboxyl-terminal occlusion complex. Fraction 9 from the ion exchange purification step shown in Figure 5 was further purified via size exclusion chromatography on a Superose 12 column. The eluates were visualized by silver staining.

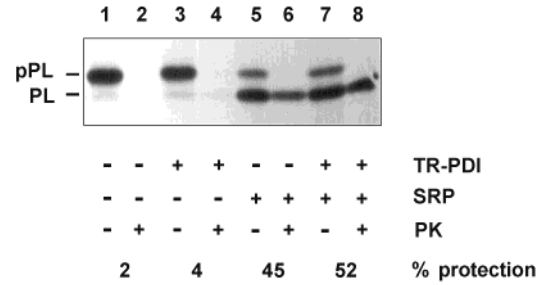

FIGURE 7: TR-PDI only slightly modulates the efficiency of translocation of preprolactin. Cholate-stripped microsomes were reconstituted with and without TR-PDI and added to a wheat germ cell-free translation system programmed with preprolactin mRNA and [^{35}S]methionine such that *de novo* products of the protein synthetic machinery will be radioactively labeled and therefore visualized on radiographic film after separation on an SDS−PAGE gel. Where indicated, the translations were supplemented with the signal recognition particle (SRP). Half of each translation reaction mixture was treated with proteinase K (PK) to assay for successful translocation, due to its occlusion within the lumen of the endoplasmic reticulum microsome. The intensities of the preprolactin (pPL) and the signal peptide-cleaved prolactin (PL) bands were measured by scanning densitometry. The percent protection is defined as the fraction of the total translated product (pPL + PL in the lanes without PK) that undergoes signal processing and remains inaccessible to protease (PL in the lanes with PK).

possibly replacing the signal recognition particle (SRP) by allowing post-translational translocation (which has been shown to depend on Kar2/BiP in yeast) (*29*).

In vitro translocation assays were carried out using the secretory hormone protein, preprolactin, as the translocation substrate (*30*). These assays were conducted both in the presence and in the absence of exogenous SRP. Three different membrane preparations were employed: native RER (RM), detergent-washed microsomes (ChoRM), and ChoRM reconstituted with purified TR-PDI. As shown in Figure 7, preprolactin is negligibly affected by TR-PDI, as the yield of translocated PL is only slightly higher (<10%) in the presence of TR-PDI than in its absence (compare the PK insensitive PL present in lane 6 of Figure 7 to that in lane 8). Though a negligible amount of protease-protected prolactin is translocated in the absence of SRP when TR-PDI is present (Figure 7, lanes 3 and 4), this amount of protease-protected preprolactin, which is only very slightly above background, indicates TR-PDI is not a functional substitute for the signal recognition particle.

We next tested a glycosylated type I membrane protein [vesicular stomatitis virus glycoprotein (VSVG) (*31*)] and a secretory protein that requires reinsertion into the translocon after translocational pausing, ApoB (*20*). Both showed little response to the absence of TR-PDI (data not shown). Further, the presence of TR-PDI did not increase the overall efficiency of ApoB translocation or accentuate the TRAM-dependent pausing of ApoB that has been noted by Hegde and co-workers (*32*). These results also show that mild cholate washes of these microsomal membranes leave the translocon functional and active, as the ChoRM behavior was nearly indistinguishable from the behavior of the RM membrane pool for the translocation substrates preprolactin, VSVG, and apolipoprotein B.

In the search for evidence of highly TR-PDI sensitive translocation substrates, we next screened a large pool of candidates by observing the effect of TR-PDI on the translocation of proteins derived from total canine kidney mRNA (data not shown). Because there were only two proteins from a panel of ≥100 protein translation products that displayed a change in translocation efficiency in the absence of TR-PDI, we concluded that the effect of TR-PDI on translocation across the RER is likely to be highly substrate specific.

The Prion Protein as a Translocation Substrate. Following this reasoning, we noted that it has been proposed by Hegde and Lingappa that cytosolic trans-acting factors may comprise a set of proteins that are involved in translocation, yet that only interact with particular subsets of translocation substrates (*33*). Termed "translocation accessory factors" (TrAFs) by Lingappa and Hegde, these proposed cytosolic factors are suggested to chaperone putative transmembrane domains of translocation substrates via interaction with select regions of the protein (*33*). TRAM displays this type of substrate specific behavior, though its existence as a membrane protein prevents its inclusion as a TrAF factor, *per se* (*32*). TR-PDI appeared to us to be a candidate as a trans-acting factor, because of its putative location on the cytosolic face of the translocon and our knowledge that it appears to affect a small but detectable subset of translocation substrates.

Translocation of the Prion Protein. In cell-free translocation systems, the human prion protein, PrP, can be translocated in a manner that results in three distinct topological forms (*22*). The native form of the prion protein in healthy brain tissue is fully translocated into the ER lumen, and is tethered to the membrane by a glycolipid anchor (*34*); this is termed the secretory form and is denoted ^{Sec}PrP. The prion protein can also produce two transmembrane isoforms. Each isoform has been show to span the membrane once, with either the carboxyl terminus or the amino terminus exposed to the ER lumen (*22*). The ^{Ctm}PrP isoform has been found to be highly correlative with the neurodegeneration that is the hallmark of scrapie and other neurodegenerative spongiform encephalopathies (*22*, *35*).

We postulated that production of one or more of the prion protein topologies may be dependent on the presence of TR-PDI, as proper insertion has been demonstrated to depend on detergent sensitive factors (*33*). We first chose to assay the congenital prion protein mutant AV3, which displays an

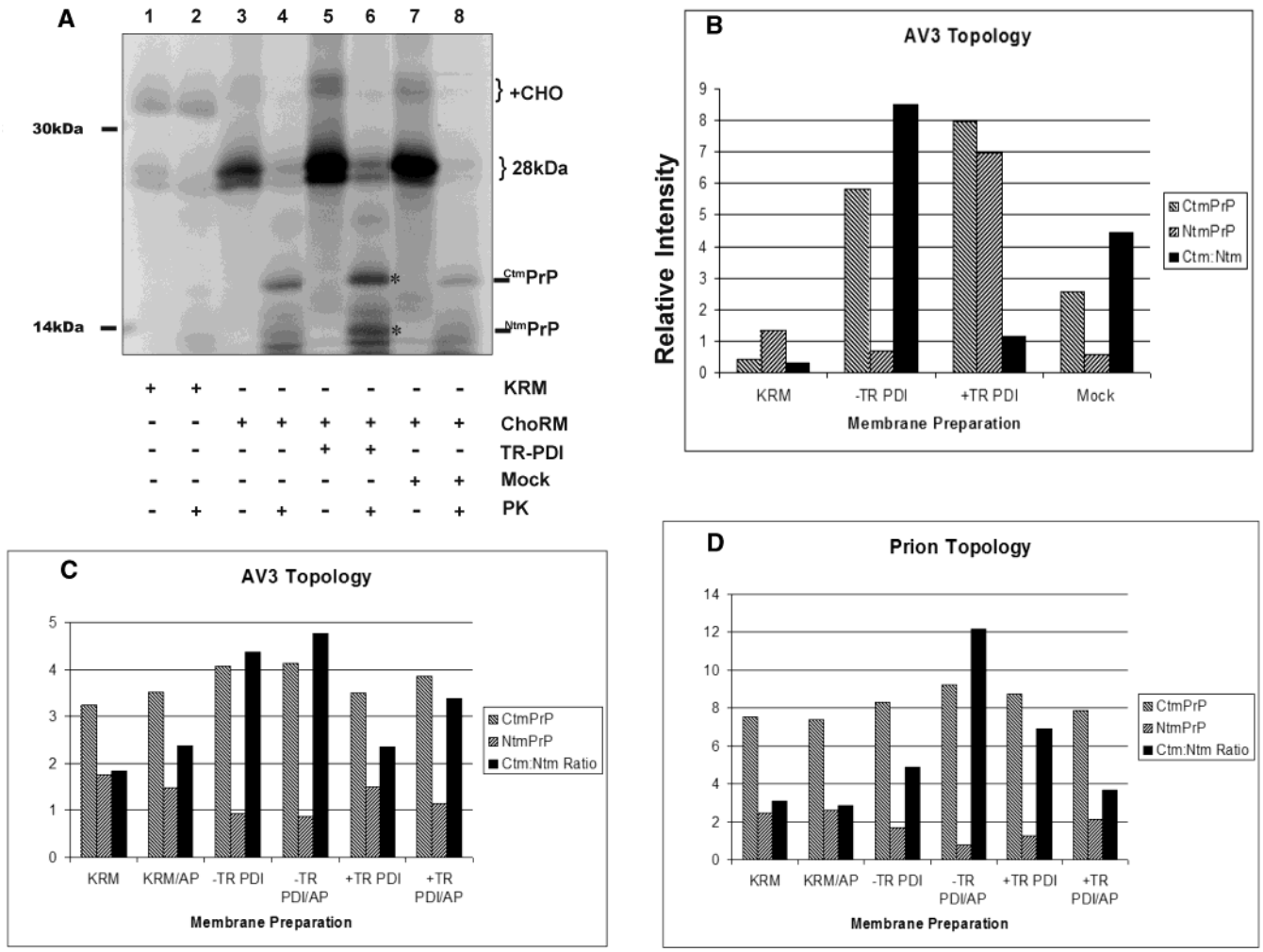

FIGURE 8: TR-PDI affects the insertion topology of the AV3 prion protein mutant and native prion protein. (A) Prion mutant AV3 was translated in a wheat germ translation system in the presence of 3 equiv of membranes. After translation and/or translocation, half of each reaction mixture was treated with 500 μg/mL proteinase K (PK) to test for the sequestration of radiolabeled protein or the presence of the two membrane insertion topologies of PrP. The locations of these 18 kDa (^{Ctm}PrP) and 14 kDa (^{Ntm}PrP) digestion products are labeled with asterisks. In lanes 1 and 2, the translation was supplemented with KRM. Lanes 3 and 4 included KRM that had been washed with 3 M NaCl and then subsequently with 0.05% sodium cholate (without TR-PDI). In lanes 5 and 6, the ChoRM used in lanes 3 and 4 was reconstituted with an excess of purified TR-PDI. In lanes 7 and 8, the ChoRM used in lanes 3 and 4 was mock-reconstituted with buffer. The products of these translations were separated on a 12 to 20% SDS gel and visualized via fluorography. The bands labeled +CHO correspond to the glycosylated form of the full-length protein. (B) The densities of the 14 kDa (^{Ntm}PrP) and 18 kDa (^{Ctm}PrP) bands were measured via scanning densitometry of the ^{35}S fluorographs; relative densities are shown. The densities of the two proteolytic products were compared, and are presented as ^{Ctm}PrP:^{Ntm}PrP ratios. The numbers on the left-hand axis refer to the relative ratios of ^{Ctm}PrP to ^{Ntm}PrP under each of the translocation conditions that is described. (C) The effect of TR-PDI on AV3 translocation is not dependent on the glycosylation machinery. The densities of the 14 kDa (^{Ntm}PrP) and 18 kDa (^{Ctm}PrP) bands were measured via scanning densitometry. The relative density of each and the ratio of the two densities (^{Ctm}PrP:^{Ntm}PrP) are plotted. (D) The densities of the 14 kDa (^{Ntm}PrP) and 18 kDa (^{Ctm}PrP) bands were measured via scanning densitometry. The relative density of each is shown, as is the ratio of the two densities (^{Ctm}PrP:^{Ntm}PrP).

enhanced propensity to misinsert, resulting in an increase in the ^{Ctm}PrP topology (*22*).

We analyzed prion insertion profiles using proteinase K digestion of the ER microsomes after insertion of the AV3 prion into the membrane, as the limit digestion product for the unglycosylated ^{Ctm}PrP has a mass of 18 kDa, whereas the limit digestion product for ^{Ntm}PrP has a mass of 14 kDa. The secreted form (^{Sec}PrP) remains full-length (28−36 kDa, depending on the glycosylation state) due to full occlusion in the ER lumen.

In agreement with the results of Hegde and co-workers, AV3 translated in the presence of KRM and subsequently treated with proteinase K to reveal the topologies of the PrP products displayed the glycosylated, fully secreted ^{Sec}PrP form, visible as a light banding at ~36 kDa (Figure 8A, lanes 1 and 2). The 14 kDa ^{Ntm}PrP digestion fragment and the 28 kDa secreted, nonglycosylated forms were negligible in the presence of KRM (Figure 8A, lanes 1 and 2), but became visible when cholate-washed RM were used (Figure 8A, lanes 3−8). Further, when the membranes were washed of protein components sensitive to 0.05% cholate, including TR-PDI, the most abundant limit digestion product became the incorrectly inserted 18 kDa ^{Ctm}PrP fragment (Figure 8A, lane 4). These membranes produced very little of the fully translocated prion protein AV3 substrate (seen as a lack of translation products at 28 and 36 kDa; Figure 8A, lane 4). We also noted that the cholate wash had a positive overall effect on the total translation rate for the prion protein (Figure

8A, lane 3), a behavior we commonly observe when membranes are subjected to treatments such as high-salt washes that remove select subsets of membrane-associated proteins (unreported observations).

To determine if TR-PDI is responsible for the observed changes in PrP insertion topology, ChoRM membranes were then reconstituted with the purified TR-PDI component from the cholate wash (+TR-PDI microsomes; Figure 8A, lanes 5 and 6). This resulted in a direct increase in the yield of both the ^{Ctm}PrP and ^{Ntm}PrP topologies, with the greatest effect on the ^{Ntm}PrP topology (Figure 8A, lane 6 vs lane 4; Figure 8B, graph). Readdition of purified TR-PDI to cholate-washed membranes also resulted in an increase in the overall translation rate, as the yield for all three prion species increased when cholate-stripped membranes were supplied with exogenous TR-PDI.

Though even mock-reconstituted membranes displayed a measurable decrease in the yield of ^{Ctm}PrP versus that seen for ChoRM, they did not display a concomitant increase in the yield of ^{Ntm}PrP; the increase in the ^{Ntm}PrP topology required the additional presence of TR-PDI (compare lane 6 to lane 8 in Figure 8A). The additional yield of the 28 kDa PrP translation product generated in the mock-reconstituted microsomes does not appear to reflect the successful engagement of the translocation apparatus when TR-PDI was not present, as the 28 kDa translation product was not protease-protected (seen as a relative lack of digestion products at 14, 18, and 28 kDa; Figure 8A, lane 8).

We considered the possibility that the relative increase in the abundance of the ^{Ctm}PrP carboxyl-terminal form we observed in membranes washed of TR-PDI was artifactual, and due to changes in glycosylation rather than a change in insertion topology. As a control, the assay shown in panels A and B of Figure 8 was repeated with and without the addition of AP, a peptide inhibitor of N-linked glycosylation (*36*), to distinguish these two possibilities. This also afforded much more visible translation products for the full-length PrP in the control lanes (seen as a lack of clearly visible products in lanes 1 and 2 of Figure 8A due to diffuse banding of the variably glycosylated full-length proteins).

The presence of AP resulted in more clearly visible full-length prion protein, but did not alter the changes in topology or the overall results (data not shown). As before, we observed an increase in the ^{Ctm}PrP topology in the absence of TR-PDI, and a relative increase in the ^{Ntm}PrP topology when TR-PDI was reconstituted onto the microsomal membranes (Figure 8C, graph). As a control, the assay shown in panels A and B of Figure 8 was repeated with and without the addition of AP, a peptide inhibitor of N-linked glycosylation (*36*), to distinguish these two possibilities. This also afforded much more visible translation products for the full-length PrP in the control translations (data not shown).

The presence of AP resulted in more clearly visible full-length prion protein, but did not alter the changes in topology or the overall results. As before, we observed an increase in the ^{Ctm}PrP topology in the absence of TR-PDI, and a relative increase in the ^{Ntm}PrP topology when TR-PDI was reconstituted onto the microsomal membranes (Figure 8C, graph). This indicates the bands occurring at 14 and 18 kDa are the presumed ^{Ctm}PrP and ^{Ntm}PrP protease products, respectively, and not a fortuitous generation of the same molecular weight products due to a change in glycosylation. In both cases (with or without the glycosylation inhibitor AP), the reconstitution of purified TR-PDI onto cholate-stripped microsomes resulted in a relative decrease in the ^{Ctm}PrP insertion topology versus the ^{Ntm}PrP topology for prion protein translocation (Figure 8B,C).

Translocation of the Native Prion Protein. We next turned to translocation studies of the native prion protein, to determine whether the results obtained with the AV3 mutant are representative of the native translocation of the prion protein in the presence and absence of TR-PDI (Figure 8D). Translation of the native prion protein demonstrated the same trends, with the yield of ^{Ctm}PrP increasing in the absence of TR-PDI, though the overall yield of the misinserted isoforms was lower, as expected. Reconstitution of the cholate-washed membranes with TR-PDI failed to successfully restore native behavior for the ER microsomes, as the production of the fully secreted form of the prion protein (^{Sec}PrP) was not observed.

Under all circumstances (AV3 or prion translations, with and without AP glycosylation inhibitor to control for changes in glycosylation behavior, and native prion protein; Figure 8A−D), membranes that had been washed of TR-PDI along with a small subset of other proteins displayed a measurable change in prion protein insertion topologies. The most visible effect of reintroduction of purified TR-PDI to membranes subjected to mild cholate washes was a measurable increase in the relative yield of the ^{Ntm}PrP insertion topology.

DISCUSSION

Antibodies are unable to recognize and bind to the carboxyl termini of the membrane protein Sec61pα in sealed, cytosolic-side-out rough endoplasmic reticulum microsomes prior to treatment with very low concentrations (0.01−0.05%) of sarkosyl or cholate. We found that (1) the concentrations of cholate used to expose the carboxyl terminus of Sec61pα are lower than those necessary to breach the integrity of the rough ER membranes, (2) antibodies tethered against the carboxyl terminus of Sec61pα bind to the outside of intact microsomes after treatment with detergent, (3) microsomes that are immunoprecipitated with the tethered anti-Sec61α antibodies also contain OST48, indicating the microsomes remain intact, and (4) the cholate extract has the ability to re-occlude the Sec61α epitope. For these reasons, we feel the location of the carboxyl terminus of Sec61pα is indeed cytosolic, yet is occluded in these stringently washed RER microsomes that are fully active in translocation (*1*). This behavior led us to the isolation of a complex of proteins that are able to re-occlude Sec61pα from the cytosolic face of cholate-washed RER membranes. We have named this complex TR-PDI.

The identity of the proteins in this complex (PDI, BiP, and PDI family members ERp72 and CABP1/P5) was completely unexpected, as these proteins are primarily known for their high abundance in the lumen of the rough endoplasmic reticulum.

The experiments described in these studies assume that the composition of our RER microsomes, prepared by the standard method used in this field of study, accurately represents the composition of the native RER membrane. Our data suggest that this complex exists in a near-stoichiometric ratio with respect to Sec61pα in the membrane, as less than 0.01% of available anti-Sec61pα IgG

binding is realized in native microsomes, yet mild cholate washing to remove a select group of proteins, including TR-PDI, produces Sec61pα epitope exposure that is comparable to that of the fully accessible SRP54 epitope. The observation that maximal binding of anti-SRP54 antibodies to these same RER microsomes occurs in the absence of detergent treatment indicates that these are natively symmetric, right-side-out microsomes, and that there is no artifactual occlusion of surface protein complexes such as SRP54.

While it not possible to establish that the process of RER microsome generation does not result in artifactual redistribution of proteins with respect to sidedness of the microsomal membrane, these membranes are robust in their ability to translocate and fully protect translocation products, and do not release other highly abundant lumenal proteins until stronger detergent treatments are employed. Further, highly abundant lumenal chaperones such as calnexin, calreticulin, and GRP94, which are known to be copurified with PDI, BiP, CABP1/P5, and ERp72, are notably absent from TR-PDI, arguing that this complex is not the result of artifactual isolation of highly abundant chaperones that have leaked from the lumen of the RER.

The relative intensities of the bands in ion exchange fractions 7−9 (Figure 5A) are different from one ion exchange fraction to the next, suggesting that these proteins do not constitute a complex with a single, fixed composition. However, all four bands behave as a single oligomeric complex when separated by size exclusion chromatography despite their differences in apparent molecular weight (Figure 6). This strongly suggests that this collection of four proteins remains associated with one another during the chromatographic separation under the conditions that are employed. We feel that TR-PDI isolated from the cytosolic face of Sec61pα is physiologically meaningful, as its behavior (occlusion of Sec61pα) correlated with this specific set of proteins that comigrated on two different separation profiles.

Novel Location. Historically, PDI has been identified as a lumenal protein based largely on the existence of a carboxyl-terminal ER retention sequence, immunofluorescent localization studies, latency of activity, and the fact that PDI is extracted from endoplasmic reticulum-derived microsomes using mild detergents or alkaline pH (*37*, *38*). However, even mildly basic wash conditions, such as the pH 9.1 wash employed by Bulleid and Freedman (*39*), are capable of removing >90% of the PDI activity from microsomal vesicles. A significant amount of PDI can be removed from sealed pancreatic RER vesicles at pHs as low as 7.5 (*40*), and it has been further noted that 40−60% of PDI activity in dog pancreatic microsomes is accessible *without* prior detergent treatment of the sealed vesicles (*40*).

CABP1/P5, PDI, BiP, and ERp72 all contain consensus carboxyl-terminal ER retention sequences (H/K-D/E-E-L), though we cannot determine if the isoforms isolated here contain these cognate carboxyl termini. However, the presence of KDEL-type retention sequences would not, in any case, require that these exist in the lumen, as this ER retrieval sequence appears to be neither necessary nor sufficient for ER residency (*41*, *42*).

Several other PDI family members have also been found in non-RER compartments in the cell, some with and some without ER retention signals (*43*, *44*). TR-PDI therefore appears to be the newest member of a growing family of PDI proteins that do not reside solely in the ER and which may or may not contain KDEL sequences. It may represent a subpopulation of BiP and PDI family members that remain cytosolic throughout their lifetime and possess an activity specific to this location. Sequence data from the CABP1/P5 protein in purified TR-PDI reveal a peptide corresponding to an uncleaved putative signal sequence. This suggests that the CABP1/P5 protein in TR-PDI has never been a substrate for the translocon itself, and therefore has not been exposed to the signal peptidase resident on the lumenal side of the rough ER. Similarly, it has been suggested by others that ERp60, a protein disulfide isomerase isoform found variously in the plasma membrane, cytosol, and nucleus (*45*−*47*), carries out different functional roles in the cell related to its location (*48*).

In yeast, PDI-1 is the only member of the five PDI-like proteins that is required for cell survival. Deletion of the other four PDI family members has been found to affect cells only under stress conditions, making deletion mutants of these PDI family members more sensitive to chemical assault (*42*). For this reason, we propose that TR-PDI may exhibit chaperone-like activity that can only be observed *in vitro* if the translocation substrate is highly likely to misfold or misinsert in its absence.

The Ribosome−Translocon "Gap". Cryoelectron microscopy of actively translocating RER membrane-bound yeast ribosomes displays a controversial 15−20 Å gap between the ribosome and the cytosolic surface of the Sec61p "tunnel" (*49*, *50*). It has been suggested by others that this gap does not accurately depict ribosome−translocon interactions that occur in native RER membranes, due to removal of cytosolically disposed protein components during the detergent treatment used to prepare samples for microscopy (*51*). Indeed, it is difficult to envision how a regulated, tight junction can be maintained at the ribosome−translocon junction if the gap is present *in vivo*. The location of TR-PDI supports a model in which TR-PDI binds at this ribosome−Sec61p interface (see Figure 9), filling the intuitive need for additional components to create a seal between the cytosol and the interior of the translocon (*2*, *52*).

TR-PDI as a Dynamic Shuttle. During translocation, the ribosome is able to elicit large-scale reorganization of the translocon when it detects a full-length transmembrane segment of the translocating substrate. This binding results in sealing of the translocon by BiP, and a change in the internal diameter of the translocon from a 40−60 Å pore to a 9−15 Å pore (*52*). Johnson and co-workers suggest that a translocon protein extends into the ribosome nascent chain tunnel, perhaps even far enough to contact the TM segment directly while it resides within the ribosome. TR-PDI components may be candidates for accompanying nascent polypeptides into the translocon pore, which would contribute to the observed conformational change (*53*). A similar, unknown protein is seen in *Escherichia coli* translocation intermediates, as Nissen and co-workers detected an elongated protein adjacent to the nascent chain tunnel in the large ribosomal subunit of the 50S subunit of bacterial ribosomes (*54*).

Behavior of Specific Members of TR-PDI. BiP, which is a member of TR-PDI, has been noted as a central component in translocation, as it coordinates precursor docking, pore insertion, and release of the nascent chain into the lumen of

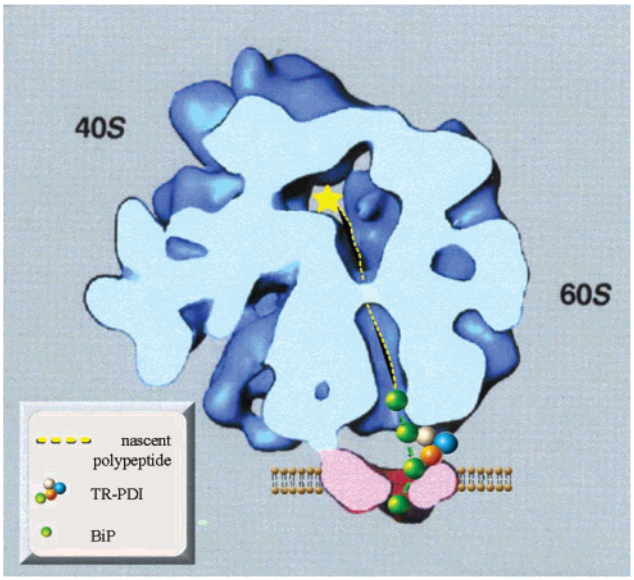

FIGURE 9: Model for interaction of BiP and TR-PDI with the translocon pore. Cross section of canine ribosome image obtained from cryoelectron spectroscopy (*62*). The location of the tRNA binding site is indicated with a yellow star. Cytosolic TR-PDI is depicted as a protein complex that both seals the ribosome−Sec61p juncture and occludes the carboxyl terminus of Sec61pα from exogenous antibody interactions. BiP may behave as a shuttle, following the translocating nascent polypeptide into the interior of the translocon pore, resulting in a smaller internal diameter for the translocon during the translocation event. BiP that resides on the lumenal side of the translocon may be a result of this shuttling process, or it may be a separate pool that remains at that location. Modified, with permission, from Figure 3D of Beckman et al. (*62*).

the endoplasmic reticulum (*55*). In these roles, BiP is implicated in cytosolic events of the endoplasmic reticulum (precursor docking). The existence of a cytosolic BiP helps to make sense of previously reported results that have been difficult to incorporate into current models of translocation. In yeast, Sanders and co-workers found that Kar2 (BiP) functions at an early, undefined step in yeast post-translational translocation, in addition to its role as a lumenal chaperone (*55*). In that study, it was reported that BiP mediates the ATP-dependent substrate release from a complex consisting of Sec62, Sec71, and Sec72 into the Sec61 translocon pore (*55*). The ability of a presumed lumenal protein (BiP) to affect a transport event on the cytosolic side of the membrane is a confounding result. The physical presence of a complex that includes BiP on the cytosolic side of Sec61p, either as a permanent resident or as part of a dynamic shuttling mechanism, helps makes sense of these results.

BiP also acts as a permeability barrier for agents that are introduced on the cytosolic side of RER membranes. Johnson and co-workers have reported that specific re-addition of BiP to mammalian RER microsomes results in behaviors exhibited on the cytosolic side of microsomes, as reintroduced BiP creates a barrier between cytosolic iodide ions and translocation substrate molecules that occupy the interior of the translocon (*51*, *52*, *56*). The "seal" that BiP creates is reversible, and changes its position cyclically during the translocation of elongating substrate molecules; it also seals in a manner that is dependent on the composition of the underlying substrate sequence. These behaviors may indicate that BiP moves in and out of the translocation pore in a substrate-dependent manner.

BiP bears a striking resemblance to the bacterial translocation protein SecA, a cytosolic bacterial translocation protein that has no known mammalian counterpart. Both ratchet segments of nascent polypeptides across the membrane (*57*), are ATPases, and reside in the proximity of Sec61 or its bacterial homologue, SecY (*58*). If, indeed, BiP accompanies the translocation substrate as it ratchets the nascent polypeptide through the translocon, its existence on both the cytosolic and lumenal sides of the RER membrane would be expected. We have incorporated these observations into a proposed model of the translocon that depicts TR-PDI creating a seal at the ribosome−Sec61p interface, with at least one component (BiP) accompanying the translocation substrate during egress from the ribosome (see the model in Figure 9).

Are all four members in purified TR-PDI constitutive members of this cytosolic, Sec61pα occluding factor in the native cell? The works cited above give a strong indication that BiP indeed resides on the cytosolic face of the translocon. CABP1/P5, with its intact signal sequence, also appears to exist separate from the native lumenal protein pool, as the signal sequence would be expected to be cleaved if it were natively translocated to the RER lumen.

Though the results shown in Figure 4, and from Chris Nicchitta's laboratory, indicate that we are 10−20-fold below the cholate concentration necessary to access the lumenal compartment when we remove the occluding factor from the cytosolic face of Sec61pα, TR-PDI was purified from a pool that is only 2−4-fold lower in cholate concentration than that necessary to access lumenal components. We therefore must consider the possibility that PDI and ERp72 typically reside in the lumen of intact cells, yet have copurified with BiP and CABP1/P5.

If the complex is highly dynamic and has members on both sides of the ER membrane and the oligomeric complexation of component proteins is sufficiently strong, it is possible that ERp72 and PDI have partitioned into the cholate wash to remain associated with their cognate partners, BiP and CABP1/P5.

If this is so, we predict that the interactions between ERp72, PDI, BiP, and CABP1/P5 are physiologically relevant, yet the interaction may be displaced relative to the ER membrane. In intact cells, interaction with PDI and ERp72 may occur only with BiP and/or CABP1/P5 that has passed through the membrane. Additional experiments will be necessary to establish the temporal and spatial interactions of this complex *in vivo*.

Translocation of the Prion Protein. The human prion protein displays compelling differences in translocation behavior when cytosolic TR-PDI is washed from the RER membranes. Loss of TR-PDI by mild detergent washing of the NaKRM membranes resulted, in all cases, in perturbation of prion protein membrane insertion, with the most pronounced effect appearing as an increase in the yield of the ^{Ctm}PrP topology. Reconstitution of these membranes with purified TR-PDI resulted in a relative increase in yield for the ^{Ntm}PrP topology versus the ^{Ctm}PrP topology. We therefore believe TR-PDI may constitute the previously reported cholate-extractable component that is responsible for the prion protein topology with the amino terminus in the lumen (*33*).

Using the prion protein as a substrate to test the effects of TR-PDI is especially interesting because the ^{Ctm}PrP isoform has been shown to correlate with neurodegeneration in mice (*59*). It should be noted, however, that the presence of ^{Ctm}PrP does not itself constitute a prerequisite for cell death (*60*). Subsequent ERAD degradation of the ^{Ctm}PrP involves removal of the amino and carboxyl termini, followed by retrograde transport back to the cytosol. It has recently been shown that this cytosolic form of partially degraded prion protein (cyPrP) is extremely cytotoxic (*60*, *61*). TR-PDI may be involved in protection against cytotoxic effects of prion protein mistranslocation through its ability to decrease the level of production of ^{Ctm}PrP (possibly via involvement of the ERAD pathway).

CONCLUSIONS

Sepharose bead-tethered antibodies directed against the carboxyl terminus of anti-Sec61pα are able to pellet sealed, right-side-out RER microsomes, but only after mild cholate or sarkosyl treatment has removed a small subset of proteins from the microsomal surface. We were able to purify a factor from this subset of proteins that reversibly occludes antibody binding to Sec61pα. Peptides from the purified components of the occluding complex were identified by nano-electrospray tandem mass spectrometry as PDI, BiP, ERp72, and CABP1/P5. We have named this complex TR-PDI, due to the preponderance of PDI family members. The key location of TR-PDI, at the crux of the ribosome−Sec61pα junction, and its near-stoichiometric abundance with Sec61pα suggest that it may have a unique role in the operations of the active translocon. Changes in translocation behavior for RER microsomes that have been washed of TR-PDI were observed for a small subset of translocation substrates. In particular, changes in interactions between the prion protein and the translocon were observed when TR-PDI was absent, resulting in changes in the relative ratios of the various topologies of PrP across the RER membrane. The nature of this interaction suggests a chaperone-like behavior for TR-PDI at the ribosome−membrane junction, and near the carboxyl terminus of Sec61pα.

ACKNOWLEDGMENT

We thank J. Kyte for helpful suggestions that began the initial investigations described in this work as well as critical reading of the manuscript, E. First for helpful suggestions and critical evaluation of the manuscript, and V. Lingappa and F. Davidson for guidance. K.V.K. thanks P. S. and B. Glacken for their indispensable encouragement for getting this work to publication. This work is dedicated to the memory of P. A. Kellaris, husband of K. V. Kellaris, for his generous love and support.

REFERENCES

1. Walter, P., and Blobel, G. (1983) *Methods Enzymol. 96*, 84−93.
2. Simon, S. M., and Blobel, G. (1991) *Cell 65*, 371−380.
3. Kalies, K. U., Gorlich, D., and Rapoport, T. A. (1994) *J. Cell Biol. 126*, 925−934.
4. Walter, P., and Lingappa, V. R. (1986) *Annu. Rev. Cell Biol. 2*, 499−516.
5. Görlich, D., and Rapoport, T. A. (1993) *Cell 75*, 615−630.
6. Oliver, J., Jungnickel, B., Görlich, D., Rapoport, T., and High, S. (1995) *FEBS Lett. 362*, 126−130.
7. Voigt, S., Jungnickel, B., Hartmann, E., and Rapoport, T. A. (1996) *J. Cell Biol. 134*, 25−35.
8. Mothes, W., Jungnickel, B., Brunner, J., and Rapoport, T. A. (1998) *J. Cell Biol. 142*, 355−364.
9. Wang, L., and Dobberstein, B. (1999) *FEBS Lett. 457*, 316−322.
10. Stevens, F. J., and Argon, Y. (1999) *Semin. Cell Dev. Biol. 10*, 443−454.
11. Schnell, D. J., and Hebert, D. N. (2003) *Cell 112*, 491−505.
12. Song, W., Raden, D., Mandon, E. C., and Gilmore, R. (2000) *Cell 100*, 333−343.
13. Harlow, H., and Lane, D. (1988) *Antibodies: A Laboratory Manual*, Cold Spring Harbor Laboratory Press, Plainview, NY.
14. Kelleher, D. J., and Gilmore, R. (1997) *Proc. Natl. Acad. Sci. U.S.A. 94*, 4994−4999.
15. Rabilloud, T., Carpentier, G., and Tarroux, P. (1988) *Electrophoresis 9*, 288−291.
16. Kellaris, K. V., Bowen, S., and Gilmore, R. (1991) *J. Cell Biol. 114*, 21−33.
17. Gilmore, R., Collins, P., Johnson, J., Kellaris, K., and Rapiejko, P. (1991) *Methods Cell Biol. 34*, 223−239.
18. Connolly, T., and Gilmore, R. (1986) *J. Cell Biol. 103*, 2253−2261.
19. Connolly, T., Collins, P., and Gilmore, R. (1989) *J. Cell Biol. 108*, 299−307.
20. Chuck, S. L., Yao, Z., Blackhart, B. D., McCarthy, B. J., and Lingappa, V. R. (1990) *Nature 346*, 382−385.
21. Hegde, R. S., and Lingappa, V. R. (1996) *Cell 85*, 217−228.
22. Hegde, R. S., Mastrianni, J. A., Scott, M. R., DeFea, K. A., Tremblay, P., Torchia, M., DeArmond, S. J., Prusiner, S. B., and Lingappa, V. R. (1998) *Science 279*, 827−834.
23. Gürevich, V. V., Pokrovskaya, I. D., Obukhova, T. A., and Zozulya, S. A. (1991) *Anal. Biochem. 195*, 207−213.
24. Ausubel, F. M., Brent, R., Kingston, R. E., Moore, D. D., Seidman, J. G., Smith, J. A., and Struhl, K. (1998) *Preparation of Poly-(A)+ RNA*, John Wiley & Sons, New York.
25. Eng, J. K., McCormick, A. L., and Yates, J. R., III (1994) *J. Am. Mass Spectrom. 5*, 976−989.
26. Link, A. J., Eng, J., Schieltz, D. M., Carmack, E., Mize, G. J., Morris, D. R., Garvik, B. M., and Yates, J. R., III (1999) *Nat. Biotechnol. 17*, 676−682.
27. Wilkinson, B. M., Critchley, A. J., and Stirling, C. J. (1996) *J. Biol. Chem. 271*, 25590−25597.
28. Nicchitta, C. V., and Blobel, G. (1990) *Cell 60*, 259−269.
29. Brodsky, J. L., Goeckeler, J., and Schekman, R. (1995) *Proc. Natl. Acad. Sci. U.S.A. 92*, 9643−9646.
30. Sasavage, N. L., Nilson, J. H., Horowitz, S., and Rottman, F. M. (1982) *J. Biol. Chem. 257*, 678−681.
31. Schmidt, M. F., Bracha, M., and Schlesinger, M. J. (1979) *Proc. Natl. Acad. Sci. U.S.A. 76*, 1687−1691.
32. Hegde, R. S., Voigt, S., Rapoport, T. A., and Lingappa, V. R. (1998) *Cell 92*, 621−631.
33. Hegde, R. S., Voigt, S., and Lingappa, V. R. (1998) *Mol. Cell 2*, 85−91.
34. Stahl, N., Borchelt, D. R., Hsiao, K., and Prusiner, S. B. (1987) *Cell 51*, 229−240.
35. Yost, C. S., Lopez, C. D., Prusiner, S. B., Myers, R. M., and Lingappa, V. R. (1990) *Nature 343*, 669−672.
36. Lopez, C. D., Yost, C. S., Prusiner, S. B., Myers, R. M., and Lingappa, V. R. (1990) *Science 248*, 226−229.
37. Freedman, R. B., Bulleid, N. J., Hawkins, H. C., and Paver, J. L. (1989) *Biochem. Soc. Symp. 55*, 167−192.
38. Noiva, R., and Lennarz, W. J. (1992) *J. Biol. Chem. 267*, 3553−3556.
39. Bulleid, N. J., and Freedman, R. B. (1990) *EMBO J. 9*, 3527−3532.
40. Paver, J. L., Hawkins, H. C., and Freedman, R. B. (1989) *Biochem. J. 257*, 657−663.
41. Monnat, J., Hacker, U., Geissler, H., Rauchenberger, R., Neuhaus, E. M., Maniak, M., and Soldati, T. (1997) *FEBS Lett. 418*, 357−362.
42. Nørgaard, P., Westphal, V., Tachibana, C., Alsoe, L., Holst, B., and Winther, J. R. (2001) *J. Cell Biol. 152*, 553−562.
43. Xiao, G., Chung, T. F., Pyun, H. Y., Fine, R. E., and Johnson, R. J. (1999) *Brain Res. Mol. Brain Res. 72*, 121−128.
44. Phillips, J. L., Holdengreber, V., Ben-Shaul, Y., Zhang, J., Tolan, D. R., and Hausman, R. E. (1997) *Brain Res. Dev. Brain Res. 104*, 143−152.
45. Hirano, N., Shibasaki, F., Kato, H., Sakai, R., Tanaka, T., Nishida, J., Yazaki, Y., Takenawa, T., and Hirai, H. (1994) *Biochem. Biophys. Res. Commun. 204*, 375−382.

46. Ferraro, A., Altieri, F., Coppari, S., Eufemi, M., Chichiarelli, S., and Turano, C. (1999) *J. Cell Biochem. 72*, 528−539.
47. Bourdi, M., Demady, D., Martin, J. L., Jabbour, S. K., Martin, B. M., George, J. W., and Pohl, L. R. (1995) *Arch. Biochem. Biophys. 323*, 397−403.
48. VanderWaal, R. P., Spitz, D. R., Griffith, C. L., Higashikubo, R., and Roti, J. L. (2002) *J. Cell. Biochem. 85*, 689−702.
49. Beckmann, R., Spahn, C. M., Eswar, N., Helmers, J., Penczek, P. A., Sali, A., Frank, J., and Blobel, G. (2001) *Cell 107*, 361−372.
50. Menetret, J. F., Neuhof, A., Morgan, D. G., Plath, K., Radermacher, M., Rapoport, T. A., and Akey, C. W. (2000) *Mol. Cell 6*, 1219−1232.
51. Haigh, N. G., and Johnson, A. E. (2002) *J. Cell Biol. 156*, 261−270.
52. Liao, S., Lin, J., Do, H., and Johnson, A. E. (1997) *Cell 90*, 31−41.
53. Hamman, B. D., Chen, J. C., Johnson, E. E., and Johnson, A. E. (1997) *Cell 89*, 535−544.
54. Nissen, P., Hansen, J., Ban, N., Moore, P. B., and Steitz, T. A. (2000) *Science 289*, 920−930.
55. Sanders, S. L., Whitfield, K. M., Vogel, J. P., Rose, M. D., and Schekman, R. W. (1992) *Cell 69*, 353−365.
56. Hamman, B. D., Hendershot, L. M., and Johnson, A. E. (1998) *Cell 92*, 747−758.
57. Economou, A., and Wickner, W. (1994) *Cell 78*, 835−843.
58. Joly, J. C., and Wickner, W. (1993) *EMBO J. 12*, 255−263.
59. Hegde, R. S., Tremblay, P., Groth, D., DeArmond, S. J., Prusiner, S. B., and Lingappa, V. R. (1999) *Nature 402*, 822−826.
60. Ma, J., and Lindquist, S. (2002) *Science 298*, 1785−1788.
61. Ma, J., Wollmann, R., and Lindquist, S. (2002) *Science 298*, 1781−1785.
62. Beckmann, R., Bubeck, D., Grassucci, R., Penczek, P., Verschoor, A., Blobel, G., and Frank, J. (1997) *Science 278*, 2123−2126.

BI035087Q